The TiO$_2$ Refraction Film for CsI Scintillator

C. C. Chen, C. W. Hun, C. J. Wang, C. Y. Chen, J. S. Lin, K. J. Huang

Abstract—Cesium iodide (CsI) melt was injected into anodic aluminum oxide (AAO) template and was solidified to CsI column. The controllable AAO channel size (10~500 nm) can makes CsI column size from 10 to 500 nm in diameter. In order to have a shorter light irradiate from each singe CsI column top to bottom the AAO template was coated a TiO$_2$ nano-film. The TiO$_2$ film acts a refraction film and makes X-ray has a shorter irradiation path in the CsI crystal making a stronger the photo-electron signal. When the incidence light irradiate from air (R=1.0) to CsI's first surface (R=1.84) the first refraction happen, the first refraction continue into TiO$_2$ film (R=2.88) and produces the low angle of the second refraction. Then the second refraction continue into AAO wall (R=1.78) and produces the third refraction after refractions between CsI and AAO wall (R=1.78) produce the fourth refraction. The incidence light through TiO$_2$ film and the first surface of CsI then arrive to the second surface of CsI. Therefore, the TiO$_2$ film can has shorter refraction path of incidence light and increase the photo-electron conversion efficiency.

Keywords—Cesium iodide, AAO, TiO$_2$, Refraction, X-ray.

I. INTRODUCTION

X-RAY imaging plays an important role in daily life. Imaging-type x-ray detectors are essential for applications ranging from medical x rays to ast. Digital x-ray techniques have been proposed as a technology which replaces the phosphor/film detector with a digital image detector, with the prospect of overcoming some of the limitations of film-screens in order to provide higher quality images [1]-[6].

In an X-ray detector assembly, an amorphous silicon detector substrate is coated with a vapor phase deposited X-ray scintillator material. The scintillator material generates photons isotropically from the absorption of the X-rays. Individual sensor elements include a photosensor, such as a photodiode or a phototransistor, and a conversion unit. The conversion unit converts incident x-rays into low- energy radiation, such as green light, for which the photosensors have a good sensitivity.

The first generation of x-ray image intensifier was developed in the early 1950s which is actually a vacuum photoelectron imaging device built up on the principle of first converting the x-ray image into a visible light image by use of a converting screen. From the late 1960s to the early 1970s, a converting screen of CsI(Na) was developed with which both spatial resolution and x-ray converting efficiency are improved significantly. The Cesium Iodide (CsI) scintillator material is known to be a very hydroscopic salt. Exposure of the CsI scintillator material to moisture can cause the CsI scintillator material to absorb the moisture, which further causes the individual CsI scintillator needles to fuse together.

Since a regular scintillator has no function to guide the path of x-ray through, partitions functioning as a scattering surface and/or a reflection surface are required. In this paper, we provided a structure which has a function to guide the path of x-ray into Charge Coupled Device (CCD) [7]-[9].

II. EXPERIMENTAL PROCEDURE

AAO templates with pore sizes of 10 to 500 nm were generated by anodizing a commercial aluminum (Al) substrate (99.7%) in acid solutions of sulfuric acid (H$_2$SO$_4$), oxalic acid (COOH)$_2$, or phosphoric acid (H$_3$PO$_4$). The Al substrate was first ground to #1000 by SiC waterproof paper and then annealed in an air furnace at 550°C for 1 hr. The sample was then electro-polished in a bath consisting of 15 vol.% perchloric acid (HClO$_4$, 70%), 70 vol.% ethanol (C$_2$H$_6$O, 99.5%), and 15 vol.% monobutylether ((CH$_3$(CH$_2$)$_3$OCH$_2$CH$_2$OH), 85%) with a charge of 42 volts (DC) applied for 10 min, using a platinum plate as a counter.

A 20 nm pore diameter template was then fabricated by anodizing the polished-Al substrate at 18 V in 10 vol.% H$_2$SO$_4$ at 15°C for 20 min, which was the first anodization. In order to obtain an orderly pattern on the substrate for the second anodization, the first anodization film was removed in 1.8 wt.% chromic acid (CrO$_3$) + 6 vol.% H$_3$PO$_4$ solution at 60°C for 40 min. The resulting substrate, with a regular pattern on the surface, was used for the second anodization for several hours to form AAO film with various thicknesses. Finally, the sample was put in 5 vol.% H$_3$PO$_4$ at 25°C for 5 to 20 min. The nanotubes were widened to an ordered array and a good quality of Al$_2$O$_3$ NT film with 10 to 50 nm pore sizes. Similar to the above process, for 40 to 90 nm pore diameter Al$_2$O$_3$ NT template, the electrolyte was 3 vol.% (COOH)$_2$ at 25°C, and the applied voltage was 40 V. The duration of pore widening was 10 to 90 min. For 180 to 500 nm pore diameter AAO template, the electrolyte was 1 vol.% H$_3$PO$_4$ at 0°C, and the applied voltage was 200 V. The duration of pore widening was between 30 to 200 min. AAO pore diameter, length, and pore density can be controlled in the range of 10-500 nm, 0.1-200 μm, and 10^8-10^{12} tubes.cm^{-2}, respectively.

The TiO$_2$ nano-film was prepared by immersing Al$_2$O$_3$ template in titanium fluoride (TiF$_4$) pH=1.3 solution for 10 min than pH=3.0 solution for 30 min at 25°C, followed by

C. C. Chenr, C. J. Wangr, and C. Y. Chenr are with the Department of Energy Engineering, National United University, Miaoli, Taiwan (phone: +886-37-382383; fax: +886-37-382-391; e-mail: ccchen@nuu.edu.tw, egg00135@gmail.com, chen6563@gmail.com).

C. W. Hun is with the Department of Department of Mechanical Engineering, National United University, Miaoli, Taiwan (phone: +886-37-382309; fax:+886-37-382-326; e-mail: monger@nuu.edu.tw).

J. S. Lin is with the Department of Mechanical Engineering, National Chin-Yi University of Technology, Taichung, Taiwan (phone: +886-4-23924505 ext 7174; fax: +886-4- 23930681; e-mail: linjsh@ncut.edu.tw).

K. J. Huangr is with the Chung-Shan Institute of Science and Technology, Taoyuan 325, Taiwan (e-mail : kjhuang@gmail.com).

World Academy of Science, Engineering and Technology
International Journal of Chemical and Molecular Engineering
Vol:9, No:5, 2015

annealing at 450°C for 0.5 h to obtain a well adhesive TiO$_2$ film in the Al$_2$O$_3$ template.

III. RESULTS AND DISCUSSION

Light speed in vacuum is about c = 3x10^8 m/s, the air enters after really light material which slows down, resulting in the phenomenon of the refractive index. If the index of refraction of light in a vacuum is 1, the light in a variety of material refractive index is greater than 1. The air really light into the material of its velocity becomes v, the refractive index n of the material with respect to the frequency of light is n= c/v. When the two media are compared, the larger the refractive index is called optically denser medium, the smaller one is called light sparse media. The same media of different light wavelengths have different refractive indices. In the medium transparent to visible light, the refractive index normally decreases with increasing wavelength that is the red light has a smaller refractive index but, the violet has a larger refractive index in the visible light.
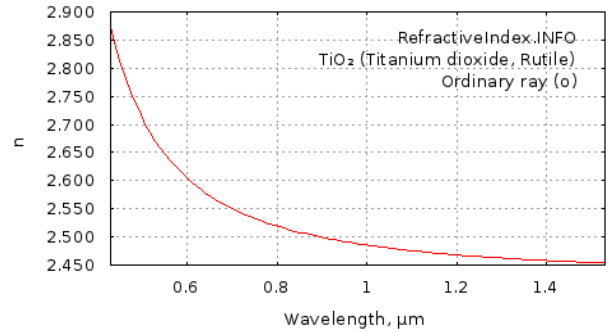
Fig. 1 showed the refractive index curves in the 200 to 1500 nm; the refractive indexes of Al$_2$O$_3$, CsI, and TiO$_2$ are 1.781, 1.838, and 2.871 at 420 nm. Because the Al$_2$O$_3$ and CsI have a similar refractive index values the X-ray becomes to penetrate Al$_2$O$_3$ and CsI interface, easily. In order to increase the light path in the CsI crystal we deposited a refraction film of TiO$_2$ which has refraction index of 2.871 on the AAO inner wall. Therefore, TiO$_2$ film acts a refraction film and makes X-ray has a shorter irradiation path in the CsI crystal and makes stronger the photo-electron signal.
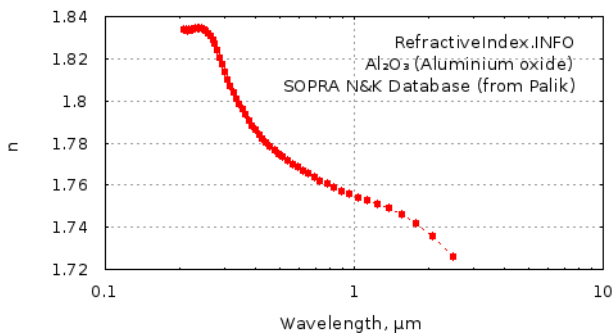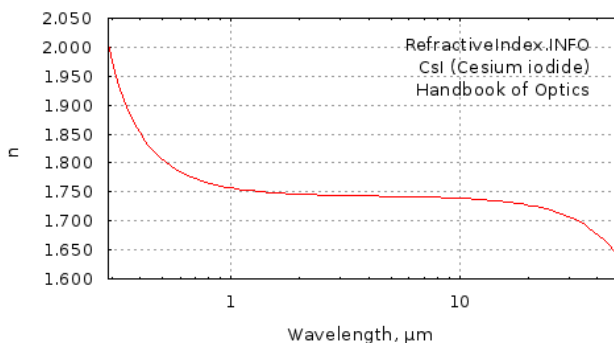
(c)

Fig. 1 The refractive index curves in the 200 to 1500 nm; the refractive indexes of Al$_2$O$_3$, CsI, and TiO$_2$ are 1.781, 1.838, and 2.871 at 420 nm
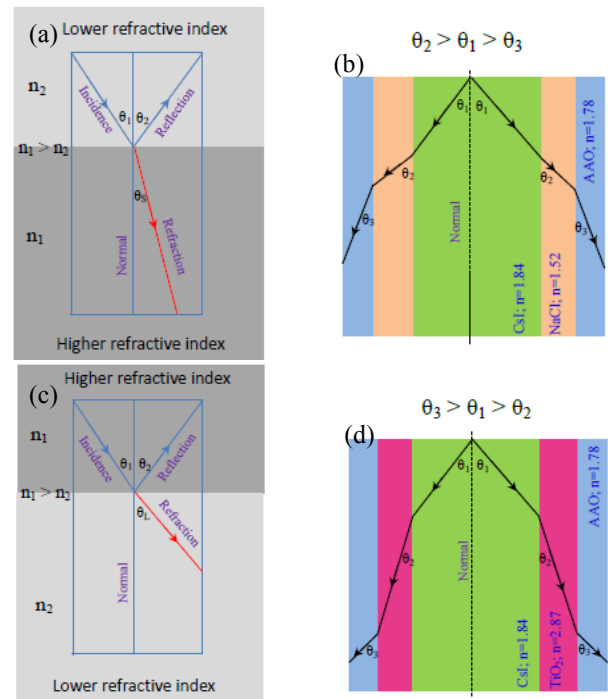

Fig. 2 Light refraction path in the various materials (a) The refraction light has a small reflection angle, (b) the incidence light is difficult go to the bulk bottom, (c) The refraction light has a large reflection angle, (d) the incidence light is easy go to the bulk bottom

Fig. 2 showed the schematic diagrams of light path in the CsI/NaCl/Al$_2$O$_3$ and CsI/TiO$_2$/Al$_2$O$_3$. The refractive indexes are 1.84/1.52/1.78 and 1.84/2.87/1.78, respectively. The incidence light from a large refractive index of the optical density of the medium into a smaller refractive optical sparse medium, refraction of light will deviate from the normal pat; on the other hand, light will be near normal path. (a) When the incidence light from a lower to a higher refractive index materials the refraction light close to the normal line. (b) Light refraction path in the CsI/NaCl/AAO composite. (c) When the incidence light from a higher to a lower refractive index materials the refraction light far to the normal line. (d) Light refraction path in the CsI/TiO$_2$/AAO composite.

Fig. 3 showed the light refraction path in the CsI. Fig. 3 (a),

(a)

(b)

World Academy of Science, Engineering and Technology
International Journal of Chemical and Molecular Engineering
Vol:9, No:5, 2015

when the incidence light irradiate from (❶) air (R=1.0) to CsI's first surface (R=1.84) the first refraction happen (❷), the first refraction continue into AAO wall (R=1.78) and produces the second refraction (❸), after refractions between CsI and AAO wall (❹, ❺, ❻, ❼, ❽) the incidence light arrive to the CsI's second surface. The more times refraction happen the longer incidence light path needed which causes the lower photo-electron conversion efficiency decreases.

Fig. 3 (b), when the incidence light irradiate from (❶) air (R=1.0) to the CsI's first surface (R=1.84) the first refraction happen (❷), the first refraction continue into TiO_2 film (R=2.88) and produces the low angle of second refraction (❸). And, then the second refraction continue into AAO wall (R=1.78) and produces the third refraction (❸) after refractions between CsI and AAO wall (R=1.78) produce the fourth refraction (❹). The incidence light after through CsI (❺) and TiO_2 film refractions (❻) arrive to the CsI's second surface. Therefore, the TiO_2 film can shorter the refraction path of incidence light and increase the photo-electron conversion efficiency.
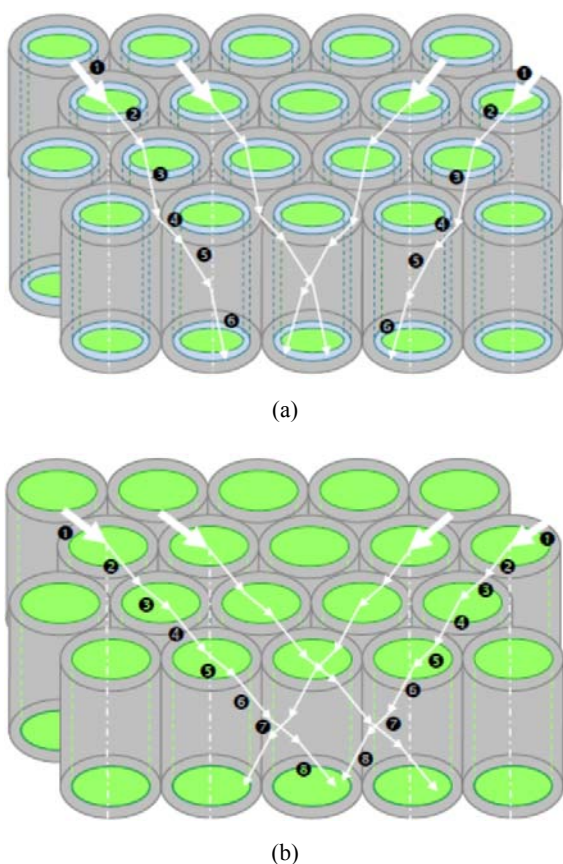

(a)

(b)

Fig. 3 Light refraction path in the (a) CsI/AAO and (b) CsI/TiO_2/AAO composites. A higher refractive index material of TiO_2 film reduces the refraction path from the CsI top to the bottom

Fig. 4 showed the TiO_2, $Ti(OH)_4$, and $Ti(OH)_2^{2+}$ chemical equilibrium diagram. When the solution pH value is lower than 2.2 the $Ti(OH)_2^{2+}$ ion is prefer formation. But, When the solution pH value is higher than 2.2 the $Ti(OH)_4$ is prefer deposition. The $Ti(OH)_4$ is beginning formation of

nano-particle form on the substrate then a continue film type and a tube type after a lasting immersion. Therefore, the form of $Ti(OH)_4$ deposition on the AAO pore wall can be controlled to a nano-particle type, a nano-film type, or a nano-tube type based on the immersion time.

According to [10]-[12], when TiF_4 solutions have a pH below 1.0 or a TiF_4 concentration below 0.03 M; neither precipitation nor film formation is observed. A large amount of precipitate is rapidly formed and film is not deposited on substrates with pH above 3.1. Therefore, the concentration of TiF4 should be controlled above 0.03 M, and the pH value should be controlled between 1 and 3 so that TiO_2 nanoparticles can present and be deposited on the substrate. For example, Chen [13] used pH 1.8, 0.04 M TiF_4 solution at 60°C for deposition on TiO_2 NT in AAO membrane.

Fig. 5 showed SEM images of TiO_2 forming in/on the AAO pore wall. When AAO is immersed in the TiF_4 solution for a shorter the $Ti(OH)_4$ film form on the AAO pore wall. When AAO is immersed in the TiF_4 solution for a longer the $Ti(OH)_4$ tube form on the AAO pore wall. For example, Fig. 5 (a) showed TiO_2 tube forming inside AAO tube under 0.2 wt.% TiF_4 solution for 2 h conditions. Fig. 5 (b) showed TiO_2 film coating on the AAO tube under 0.01 wt.% TiF_4 solution for 0.5 h conditions.

In order to observe the CsI column inside AAO-TiO_2 template the following experiment steps were needed. **(1)** CsI ingot put on the AAO surface, **(2)** heating CsI/ AAO-TiO_2 template at 630 °C, applied a hydraulic pressure (100 kgf/cm^2) to the CsI melt, **(3)** cooling CsI/ AAO-TiO_2 template sample at 30 °C/min of cooling rate. According to above steps we can obtain the CsI column inside AAO-TiO_2 template, as showed in the Fig. 6.

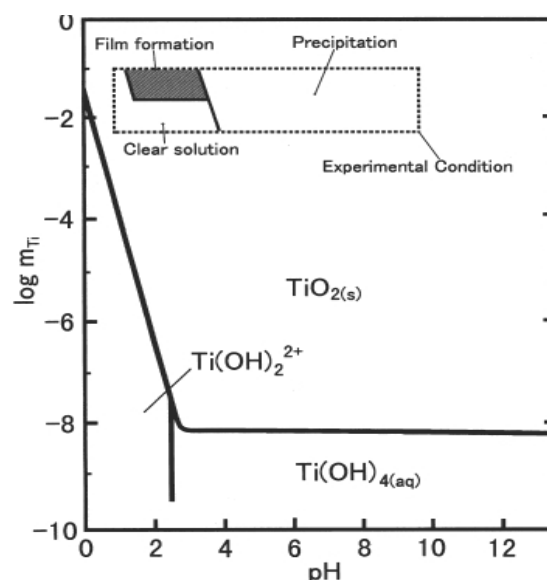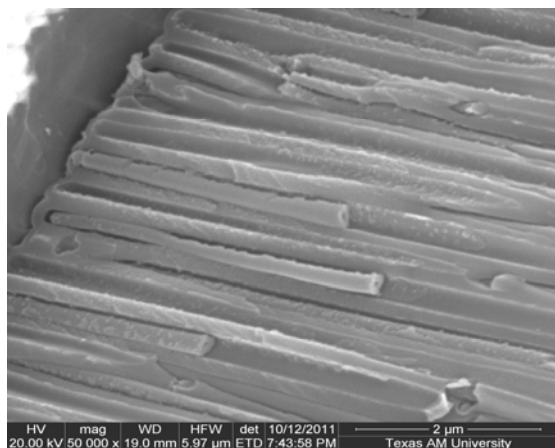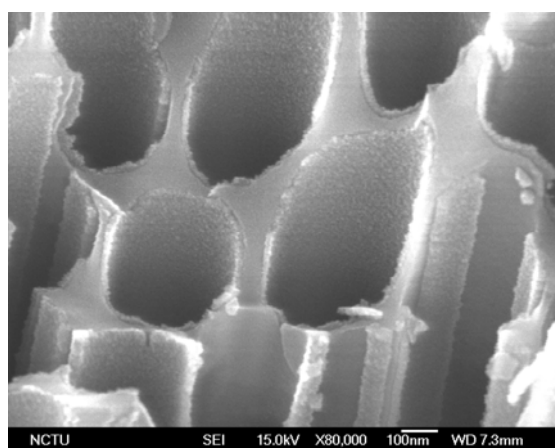Fig. 4 TiO_2, $Ti(OH)_4$, and $Ti(OH)_2^{2+}$ chemical equilibrium diagram

World Academy of Science, Engineering and Technology
International Journal of Chemical and Molecular Engineering
Vol:9, No:5, 2015

(a)

(b)

Fig. 5 SEM images of TiO$_2$ forming in/on the AAO pore wall; (a) TiO$_2$ tube forming inside AAO tube under 0.2 wt.% TiF$_4$ solution for 2 h conditions, (b) TiO$_2$ film coating on the AAO tube under 0.01 wt.% TiF$_4$ solution for 0.5 h conditions
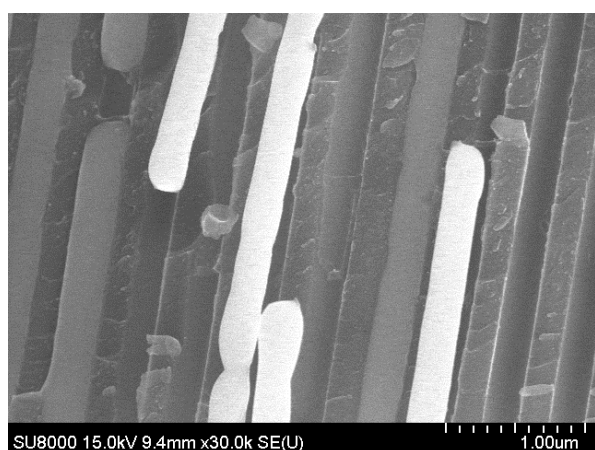

Fig. 6 SEM image of CsI column inside AAO template

IV. CONCLUSIONS

In this paper, we provided a good quality CsI column as a scintillator material. The fabrication method, including:

fabricated an anodic aluminum oxide (AAO) as a template, deposited TiO$_2$ nano-film as a refraction layer, and injected CsI melt into template formation CsI column. The TiO$_2$ film has refraction index of 2.871 which is far differences than Al$_2$O$_3$ of 1.781 and CsI of 1.838 at 420 nm wavelength. Therefore, TiO$_2$ film acts a refraction film and makes X-ray has a shorter irradiation path in the CsI crystal. The AAO having pore size from nano- to sub-micron size which means the CsI crystal can be controlled from nano- to sub-micron column.

REFERENCES

[1] C.M. Schaefer-Prokop, D.W. De Boo, M. Uffmann, M. Prokop. DR and CR: Recent advances in technology, European Journal of Radiology, 72(2), (2009) 194-201.
[2] A. Koch, C. Raven, P. Spanne, A. Snigirev, X-ray imaging with submicrometer resolution employing transparent luminescent screens, Journal of the Optical Society of America A, 15(7), (1998) 1940-1951.
[3] S Zazubovich. Physics of halide scintillators, Radiation Measurements, 33(5), (2001) 699-704.
[4] U.L. Olsen, X. Badel, J. Linnros, M. Di Michiel, T. Martin, S. Schmidt, H.F. Poulsen, Development of a high-efficiency high-resolution imaging detector for 30–80 keV X-rays, Nuclear Instruments and Methods in Physics Research Section A: Accelerators, Spectrometers, Detectors and Associated Equipment, 576(1), (2007) 52-55.
[5] A. M. Gurvich, Luminescent screens for mammography, Radiation Measurements, 24(4), (1995) 325-330.
[6] A Koch, H Rosenfeldt, Powder-phosphor screens combined with interference filters for X-ray imaging with increased brightness, Nuclear Instruments and Methods in Physics Research Section A: Accelerators, Spectrometers, Detectors and Associated Equipment, 432(2-3), (1999) 358-363.
[7] M. Stampanoni, G. Borchert, P. W., R. Abela, B. Patterson, S. Hunt, D. Vermeulen,.P. Rüegsegger, High resolution X-ray detector for synchrotron-based microtomography, Nuclear Instruments and Methods in Physics Research Section A: Accelerators, Spectrometers, Detectors and Associated Equipment, 491(1-2), (2002) 291-301.
[8] A. Ananenko, A. Fedorov, A. Lebedinsky, P. Mateychenko, V. Tarasov, Y. Vidaj, structural dependence of CsI(Tl) film scintillation properties, Semiconductor Physics, Quantum Electronics & Optoelectronics, 7(3), (2004) 297-300.
[9] E. Zych, C. Brecher, and H. Lingertat, Depletion of high-energy carriers in YAG optical ceramic materials, Spectrochimica Acta Part A: Molecular and Biomolecular Spectroscopy, 54(11), (1998) 1771-1777.
[10] H. Imai, Y. Takei, K. Shimizu, M. Matsuda, and H. Hirashima, Direct preparation of anatase TiO$_2$ nanotubes in porous alumina membranes, Journal of Materials Chemistry, 9(12), (1999) 2971-2972.
[11] H. Imai, M. Matsuta, K. Shimizu, H. Hirashima, and N. Negishi, Preparation of TiO$_2$ fibers with well-organized structures, Journal of Materials Chemistry, 10, (2000) 2005-2006.
[12] K. Shimizu, H. Imai, H. Hirashima, and K. Tsukuma, Low-temperature synthesis of anatase thin films on glass and organic substrates by direct deposition from aqueous solutions, Thin Solid Films 351(1-2), (1999) 220-224.
[13] C. Chen, C. Cheng, G. Tang, T. Lin, C. Lin, "Template Assisted Fabrication of TiO$_2$ and BaTiO$_3$ Nanotubes", Applied Mechanics and Materials 271-272, (2013) 107-111.